Functionalization of Graphene Grown on Metal Substrate with Atomic Oxygen: Enolate vs Epoxide

Jaehoon Jung, Hyunseob Lim, Junepyo Oh, and Yousoo Kim*

Surface and Interface Science Laboratory, RIKEN, Wako, Saitama 351-0198, Japan

S *Supporting Information*

ABSTRACT: Graphene functionalization is of great importance in applying graphene as a component in functional devices or in activating it for use as a catalyst. Here we reveal that atomic oxidation of epitaxial graphene grown on a metal substrate results in the formation of enolate, i.e., adsorption of atomic oxygen at the on-top position, on the basal plane of a graphene, using periodic density functional theory calculations. This is striking because the enolate corresponds to the transition state between the epoxides on free-standing graphene and on graphite. Improved interfacial interaction between graphene and the metal substrate during atomic oxidation makes the graphene enolate a local minimum and further highly stabilizes it over the graphene epoxide. Our results provide not only a novel perspective for a chemical route to functionalizing graphene but also a new opportunity to utilize graphene enolate for graphene-based applications.

Functionalization of graphene has attracted great scientific interest, not only in controlling the physical properties of graphene, e.g., opening band gap to achieve semiconducting nature, but also in improving chemical adaptability to integrate graphene as a building block into a variety of functional devices.[1] Due to the great simplicity of the atomic species, atomic functionalization on the basal plane of graphene with covalent bonds is considered a promising way to maximize the usefulness of graphene.[1d] Hydrogen,[2] fluorine,[3] and oxygen[4] have been extensively studied as key species to induce symmetry breaking of graphene composed of sp^2-hybridized carbons. In particular, atomic oxidation allows compositional expandability through additional chemical reactions. At the limit of low coverage, whereas hydrogen or fluorine makes a single covalent bond with a C atom, i.e., "on-top configuration", on the basal plane of a graphene sheet, the attachment of atomic oxygen to graphene results in graphene epoxide, i.e., "bridge configuration", in which an O atom covalently interacts with two adjacent C atoms.

The existence of atomic oxygen adsorbate as an epoxy group on the basal plane of graphene grown on SiC(0001) was examined by scanning tunneling microscopy (STM) and X-ray photoelectron spectroscopy (XPS) in ultrahigh-vacuum conditions, where atomic oxygen was prepared with a hot tungsten filament.[4c] Even for graphene oxide (GO) prepared by Hummer's solution-based method, epoxy groups as well as tertiary alcohols were identified on its basal plane with solid-state NMR,[5] whereas various kinds of oxygen-containing functional groups form at the edge of GO.[6] It is thus widely accepted that atomic oxidation of graphene leads to the formation of epoxy groups on its basal plane, i.e., graphene epoxide, which is supported by a number of theoretical studies.[7]

Compared with the compositional complexity of oxygen-containing functional groups in GO, atomically oxidized graphene is expected to provide a chemically uniform circumstance for additional functionalization. The well-established approach is nucleophilic ring-opening of epoxides.[6a,8] It was also recently reported that epoxy groups produced by atomic oxidation of graphene can be utilized to activate graphene for the growth of metal oxide nanoparticles.[9] However, other possibilities besides an epoxy group on the basal plane of graphene have been excluded, narrowing the choices of a chemical route not only for further functionalization but also for the development of graphene-based catalysts.

In this Communication, we first suggest that atomic oxidation of graphene grown on a metal substrate results in the formation of graphene enolate, i.e., negatively charged oxygen adsorbed at the on-top position on its basal plane, which is strikingly different from the formation of epoxy groups on free-standing graphene and on graphite. Whereas the enolate is the transition state between two neighboring epoxides on free-standing graphene and on graphite, we reveal that the enolate group formed on epitaxial graphene on a metal substrate exists as a local minimum, and further becomes more stable than the epoxide.

To examine atomic oxidation of a graphene sheet grown on a metal substrate, we performed periodic density functional theory (DFT) calculations, at the level of local density approximation (LDA)[10] implemented in Vienna Ab-initio Simulation Package (VASP) code,[11] for graphenes epitaxially grown on Cu(111), i.e., Gr/Cu(111) (see Supporting Information for computation details). Cu has been extensively studied as an effective substrate for graphene synthesis due to not only the self-termination at a single atomic layer[12] but also the large scale, up to 30 in.[13] Computational results for Gr/Cu(111) were also compared with those for free-standing graphene and graphite. We assumed (1×1) epitaxial graphene on the Cu(111) substrate for simplicity, which leads to only 1.9% lengthening of the lattice constant of graphene at the level of LDA. Figure 1 shows the (4×4) supercell structures employed in this study. Whereas free-standing graphene has only one type of on-top site for atomic oxidation on its basal plane (Figure 1a), there are two different on-top configurations (OT1 and OT2, red and yellow dots, respectively), corresponding to the formation of graphene enolate, on graphite and Gr/Cu(111) (Figure 1b,c). The C
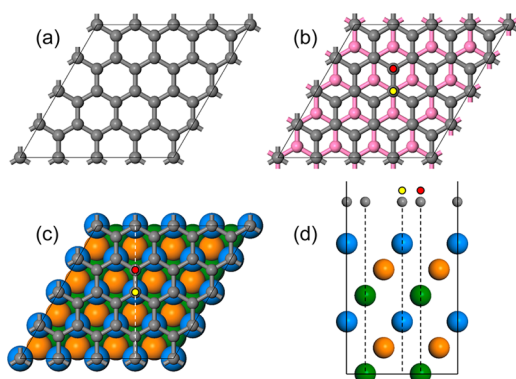
Figure 1. Simulated (4×4) supercell structures for (a) free-standing graphene, (b) graphite [first and second layers: gray and pink, respectively], and (c,d) graphene grown on metal substrate, Cu(111) [first, second, and third metal layers: blue, orange, and green spheres, respectively]. The cross-section corresponding to (d) is indicated by a dashed white line in (c). The vertical positions of C atoms with respect to metal substrate are indicated by dashed black lines in (d). Red and yellow dots indicate two different on-top configurations, OT1 and OT2, respectively, for atomic oxygen adsorbate.

Table 1. Numerical Values of Adsorption Energy (Relative Energy) for Adsorption of Atomic Oxygen on Each Adsorption Site (in eV)[a]

	Gr/Cu(111)	graphene[b]	graphite
OT1	−3.82 (0.00)	−2.39 (0.92)	−2.43 (0.87)
BR	−3.72 (0.10)	−3.31 (0.00)	−3.30 (0.00)
OT2	−3.65 (0.17)		−2.38 (0.92)

[a]Adsorption energy (relative energy) was evaluated for adsorption of single atomic oxygen in a (4×4) supercell. Negative adsorption energy indicates that atomic oxidation is thermodynamically exothermic. [b]In graphene, OT2 is identical to OT1.

atoms (β) adjacent to the oxidized C atom (α) locate at on-top and hollow sites of underneath graphite or metal layers for OT1 and OT2, respectively. Bridge configurations (BR), corresponding to the formation of graphene epoxide, are identical in each system. We considered the relative position of a graphene sheet with respect to the metal substrate reported to be the most stable (Figure 1d): half of the C atoms located at on-top sites of metal atoms and the other C atoms located at the fcc hollow site of (111) metal substrates.[14]

Atomic oxidation on graphene, graphite, and Gr/Cu(111) is exothermic because of the high reactivity of atomic oxygen, as shown in Table 1, consistent with previous computational results and experimental observations using atomic oxygen produced by thermal cracking of molecular oxygen.[1d] Whereas the formation of BR is more favorable on both graphene and graphite than adsorption at on-top sites (by ∼0.9 eV), the adsorption site preference dramatically changes on the epitaxial graphene grown on Cu(111) substrates. On Gr/Cu(111), OT1 becomes more stable than BR by 0.10 eV, although OT2 is still less favorable than BR by 0.07 eV. These results imply that the interfacial interaction between graphene and metal substrate is crucial in accounting for the stability of O adsorbate. Considering the geometric difference between OT1 and OT2 (see Figure 1), OT1 can achieve effective electronic coupling between the 2p state of C atoms and the 3d state of the metal substrate along the z-axis, especially at the β position, i.e., C atoms adjacent to C atom (α) bonding with O adsorbate.
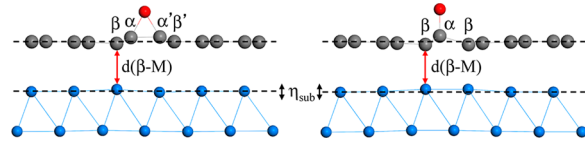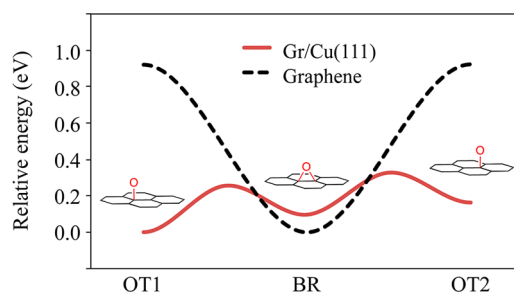

Figure 2. Potential energy surfaces for the oxygen migration between on-top (enolate) and bridge (epoxide) sites on free-standing graphene and Gr/Cu(111). The relative energy was used in constructing a potential energy surface.

We further performed frequency calculations to characterize stationary points as minima or saddle points on the potential energy landscape of O adsorbate on a graphene sheet, which unveiled a completely different situation for Gr/Cu(111) compared to graphene and graphite (see Table S1). The vibrational modes corresponding to lateral motion of O adsorbate at an on-top site are imaginary modes in both graphene and graphite, which means that OT1 (and also OT2 for graphite) is the transition state between two neighboring BRs, in agreement with previous reports.[7g] The absence of an imaginary vibrational mode for OT1 and OT2 on Gr/Cu(111) clearly indicates, however, that the graphene enolate is a local minimum on Cu(111) substrate. Thus, we examined the detailed potential energy surface for migration of O adsorbate between the on-top and bridge sites on the graphene sheet by means of climbing image nudged elastic band (CI-NEB) calculations.[15] Figure 2 clearly shows the existence of OT1 (and OT2) as a local minimum on Gr/Cu(111). The energy required for migration of O adsorbate on Gr/Cu(111), i.e., the potential energy barrier from OT1 to BR (from OT1 to OT2 through BR), is 0.26 (0.33) eV, much smaller than that on free-standing graphene (0.92 eV in this study; 0.60−0.98 eV from previous theoretical studies[4b,7f,g]). Hence, we expect that uniform arrangement of O adsorbates can be achieved at a relatively low temperature on Gr/Cu(111) substrate compared with graphene (or graphite). Our results suggest that a novel chemical route for further functionalization of graphene grown on metal substrates, beyond isolated graphene and graphite, is possible.

We present detailed information on the geometry of the optimized BR and OT1 structures to explain the influence of substrate on stabilizing the O adsorbate in Table 2. Atomic oxidations onto both graphene and graphite show almost identical results, which implies that the interaction between the topmost graphene layer and the underlying layer in graphite does not significantly affect the atomic oxidation, in accordance with the calculated adsorption energy shown in Figure 1. However, the interfacial interaction increases much during atomic oxidation on Gr/Cu(111). The geometric changes of C atoms near the O adsorbate show the critical influence of metal substrate on atomic oxidation. Whereas the positions of both α (α') and β (β') C atoms are lifted vertically by atomic oxidation for graphene and graphite, the atomic position changes in opposite vertical direction for the β C atoms on Gr/Cu(111), which approach the Cu(111) substrate by 0.07 and 0.12 Å for BR and OT1, respectively, as shown in Table 2. The considerable rumpling (η_{sub}) of the first substrate layer underneath the graphene sheet for Gr/Cu(111) also reflects the strong interfacial interaction induced by atomic oxidation (see the

Table 2. Side Views of Optimized Structures for BR and OT1, and Selected Geometric Information (in Å): Vertical Change in Atomic Position of Oxidized C Atom ($\Delta\alpha$) and Its Neighboring C Atoms ($\Delta\beta$), Rumpling (η_{sub}) of the First Substrate Layer Underneath the Graphene Sheet, and Selected Atomic Distances ($d(\beta-M)$ and $d(O-\alpha)$)[a,b]
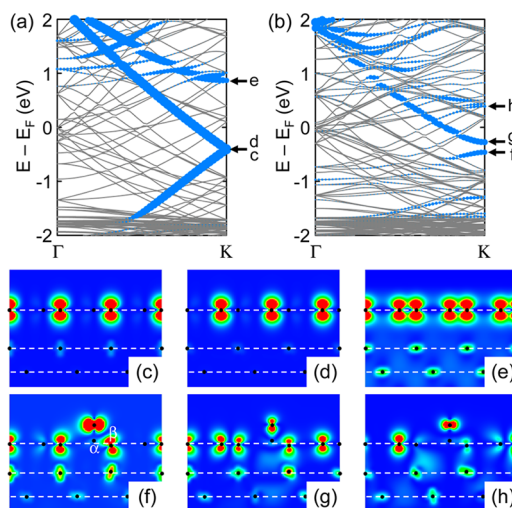

		Gr/Cu(111)	graphene	graphite
$\Delta\alpha$	BR	+0.23 (+0.25)	+0.39	+0.37 (+0.37)
	OT1	+0.31	+0.37	+0.36
$\Delta\beta$	BR	−0.07 (+0.02)	+0.12	+0.10 (+0.10)
	OT1	−0.12	+0.07	+0.05
η_{sub}	BR	0.14		0.02
	OT1	0.15		0.01
$d(\beta-M)$	bare	3.27		3.33
	BR	2.50		3.39
	OT1	2.54		3.35
$d(O-\alpha)$	BR	1.46 (1.48)	1.44	1.44 (1.44)
	OT1	1.34	1.40	1.40

[a]Δ is calculated with respect to the average z-coordinate of C atoms, except α and β C atoms. The plus sign indicates the shift up of the atomic position toward vacuum. η_{sub} is calculated from the difference between z-coordinates of highest and lowest atoms in the layer. For graphite, the second layer of the slab model is used to evaluate η_{sub}. [b]Values for α' and β' are given in parentheses for graphite and Gr/Cu(111). For BR on graphite and Gr/Cu(111), α' (α) and β (β') are located at the on-top (hollow) sites of the underlying layer.

Figure 3. Band diagrams of (a) bare and (b) OT1 Gr/Cu(111). The relative amount of C $2p_z$ character is proportional to the size of the blue dots. (c−h) Partial charge density plots for selected electronic states at **K**, for which energies are marked by black arrows in (a) and (b). Color grid for the probability of finding the electrons ranges from 0.000 (blue) to 0.005 (red) e/bohr^3. Black dots indicate the atomic positions.

side views of optimized structures), whereas the η_{sub} values in graphite are negligible. The resultant distances of β C atoms and underlying Cu atoms, $d(\beta-M)$ = 2.50 (BR) and 2.54 Å (OT1), are significantly reduced compared with the interlayer distance (3.27 Å) of bare Gr/Cu(111), which implies that the instability of a π-conjugated network induced by atomic oxidation is compensated by the enhanced interfacial interaction between graphene and Cu substrate. Interestingly, OT1 on Gr/Cu(111) shows $d(O-\alpha)$ = 1.34 Å between the O adsorbate and α C atom, which is 0.06 Å shorter, i.e., stronger, than those on both graphene and graphite. Our results can thus be explained by the higher capability of Cu(111) to stabilize the oxidized graphene compared with graphite.

Figure 3 shows the band diagrams of bare and OT1 Gr/Cu(111), and corresponding partial charge density plots at the **K**-point. It is well known that metallic substrate can alter the electronic structure of graphene, where the graphene sheet is n-type doped on Cu by charge transfer from the metal substrate to graphene.[14] For bare Gr/Cu(111), the characteristic Dirac cone in the band structure of graphene at **K** is well preserved due to physisorption, and its conical point locates at the −0.41 eV with respect to the Fermi level (E_F) (Figure 3a). Figure 3c,d shows the partial charge density for degenerated electronic states at the Dirac conical point, which indicates that the C 2p states of graphene are isolated from the electronic states of Cu(111). The higher electronic state at ∼1 eV also shows very weak electronic mixing between graphene and Cu(111) (Figure 3e). However, the electronic structure of bare Gr/Cu(111) is significantly modified by the formation of enolate on the basal plane, as shown in Figure 3b. First, the calculated band structure shows a band

gap opening of 0.18 eV. Second, the interfacial electronic couplings are strongly enhanced, as shown in Figure 3f−h, which implies that the interfacial interaction between graphene and Cu(111) changes from physisorption to chemisorption. In particular, Figure 3f,g clearly shows that the 2p states of β C atoms strongly interact with the 3d states of underlying Cu atoms at the interface.

One of the main properties tuned by functionalizing graphene is the work function. The calculated work function of Gr/Cu(111) is 4.33 eV, in good agreement with the previous theoretical value of 4.40 eV.[14a] Because the work function is significantly influenced by the charge distribution of the surface, we performed population analysis using the density-derived electrostatic and chemical (DDEC) method.[16] The calculated net atomic charges of O adsorbate are −0.50e and −0.30e for enolate and epoxide, respectively. As expected, the O atom in graphene enolate is more negatively charged than that in graphene epoxide, which is responsible for the difference in the work function of functionalized Gr/Cu(111). The computationally estimated work functions are 5.20 and 4.55 eV for OT1 and BR, respectively, on Gr/Cu(111), higher than those of bare Gr/Cu(111) by 0.87 and 0.20 eV, respectively. Considering that both configurations, OT1 and BR, are local minima for Gr/Cu(111), our results suggest that the work function of Gr/Cu(111) can be adjusted by controlling the distribution of O adsorbates.

In addition, we extended our study to epitaxial graphene grown on a Ni(111) substrate, Gr/Ni(111). Cu(111) and Ni(111) are representative metal substrates that interact weakly and strongly with graphene, respectively.[17] The geometric and electronic structures associated with atomic oxidation of Gr/Ni(111) are quite complicated compared to those for Gr/Cu(111) due to the strong chemisorption at the interface. Our DFT calculations revealed, however, that the formation of enolate is possible on Gr/Ni(111), like that on Gr/Cu(111). The adsorption energies (relative energies) of atomic oxygen on Gr/Ni(111) are −4.59 (0.00), −4.16 (0.43), and −4.10 (0.49) eV for OT1, BR, and OT2, respectively, and they are all local minima.

The stability order of atomically oxidized Gr/Ni(111) is identical to that in Gr/Cu(111). The much enhanced stability of OT1 on Gr/Ni(111) compared with Gr/Cu(111) also suggests that the interfacial interaction plays a crucial role in determining the structure of atomically oxidized graphene because of the ability of Ni(111) to have a stronger interfacial interaction with graphene. The net atomic charges of O adsorbate are $-0.58e$ and $-0.34e$ for OT1 and BR, respectively, on Gr/Ni(111), slightly larger than those on Gr/Cu(111). Accordingly, the work function of Gr/Ni(111) (3.61 eV) increases more steeply by 1.54 and 0.65 eV for OT1 and BR, respectively, compared with that of Gr/Cu(111). Our results for both Gr/Cu(111) and Gr/Ni(111) imply not only that the formation of enolate can be reasonably achieved in graphene grown on metal substrate through atomic oxidation but also that the properties of functionalized graphene can be controlled by the choice of metal substrate. Nonetheless, it is noteworthy that the recent experimental studies reported only the formation of graphene epoxide on Ir(111)[4a,b] and Pt(111),[4a] mainly using XPS. Our theoretical prediction of graphene enolate on metal substrate thus suggests revisiting the experiment with more direct approaches, such as atomically resolved STM imaging and local spectroscopy.

To summarize, our computational results strongly suggest that atomic oxidation of graphene grown on a metal substrate can provide an opportunity to extend graphene chemistry with a newly suggested functional group, enolate, on the basal plane of graphene. The interfacial interaction between graphene and metal substrate plays a crucial role not only in the formation of enolate as a local minimum but also in stabilizing it over the epoxide. Our computational study is expected to trigger experimental attempts to find the existence of graphene enolate on metal substrates and to design new chemical pathways utilizing it.

■ ASSOCIATED CONTENT

Ⓢ Supporting Information

Computation details, calculated vibrational frequencies, and fractional coordinates of optimized structures. This material is available free of charge via the Internet at http://pubs.acs.org.

■ AUTHOR INFORMATION

Corresponding Author
ykim@riken.jp
Notes
The authors declare no competing financial interest.

■ ACKNOWLEDGMENTS

■ REFERENCES

(1) (a) Rao, C. N. R.; Sood, A. K.; Subrahmanyam, K. S.; Govindaraj, A. *Angew. Chem., Int. Ed.* **2009**, *48*, 7752. (b) Georgakilas, V.; Otyepka, M.; Bourlinos, A. B.; Chandra, V.; Kim, N.; Kemp, K. C.; Hobza, P.; Zboril, R.; Kim, K. S. *Chem. Rev.* **2012**, *112*, 6156. (c) Craciun, M. F.; Khrapach, I.; Barnes, M. D.; Russo, S. *J. Phys.: Condens. Matter* **2013**, *25*, 423201. (d) Johns, J. E.; Hersam, M. C. *Acc. Chem. Res.* **2013**, *46*, 77.

(2) (a) Elias, D. C.; Nair, R. R.; Mohiuddin, T. M. G.; Morozov, S. V.; Blake, P.; Halsall, M. P.; Ferrari, A. C.; Boukhvalov, D. W.; Katsnelson, M. I.; Geim, A. K.; Novoselov, K. S. *Science* **2009**, *323*, 610. (b) Balog, R.; Jørgensen, B.; Nilsson, L.; Andersen, M.; Rienks, E.; Bianchi, M.; Fanetti, M.; Lægsgaard, E.; Baraldi, A.; Lizzit, S.; Sljivancanin, Z.; Besenbacher, F.; Hammer, B.; Pedersen, T. G.; Hofmann, P.; Hornekær, L. *Nat. Mater.* **2010**, *9*, 315.

(3) (a) Nair, R. R.; Ren, W.; Jalil, R.; Riaz, I.; Kravets, V. G.; Britnell, L.; Blake, P.; Schedin, F.; Mayorov, A. S.; Yuan, S.; Katsnelson, M. I.; Cheng, H.-M.; Strupinski, W.; Bulusheva, L. G.; Okotrub, A. V.; Grigorieva, I. V.; Grigorenko, A. N.; Novoselov, K. S.; Geim, A. K. *Small* **2010**, *6*, 2877. (b) Zbořil, R.; Karlický, F.; Bourlinos, A. B.; Steriotis, T. A.; Stubos, A. K.; Georgakilas, V.; Šafářová, K.; Jančík, D.; Trapalis, C.; Otyepka, M. *Small* **2010**, *6*, 2885.

(4) (a) Vinogradov, N. A.; Schulte, K.; Ng, M. L.; Mikkelsen, A.; Lundgren, E.; Mårtensson, N.; Preobrajenski, A. B. *J. Phys. Chem. C* **2011**, *115*, 9568. (b) Larciprete, R.; Fabris, S.; Sun, T.; Lacovig, P.; Baraldi, A.; Lizzit, S. *J. Am. Chem. Soc.* **2011**, *133*, 17315. (c) Hossain, M. Z.; Johns, J. E.; Bevan, K. H.; Karmel, H. J.; Liang, Y. T.; Yoshimoto, S.; Mukai, K.; Koitaya, T.; Yoshinobu, J.; Kawai, M.; Lear, A. M.; Kesmodel, L. L.; Tait, S. L.; Hersam, M. C. *Nat. Chem.* **2012**, *4*, 305.

(5) Cai, W.; Piner, R. D.; Stadermann, F. J.; Park, S.; Shaibat, M. A.; Ishii, Y.; Yang, D.; Velamakanni, A.; An, S. J.; Stoller, M.; An, J.; Chen, D.; Ruoff, R. S. *Science* **2008**, *321*, 1815.

(6) (a) Dreyer, D. R.; Park, S.; Bielawski, C. W.; Ruoff, R. S. *Chem. Soc. Rev.* **2010**, *39*, 228. (b) Lerf, A.; He, H. Y.; Forster, M.; Klinowski, J. *J. Phys. Chem. B* **1998**, *102*, 4477.

(7) (a) Sorescu, D. C.; Jordan, K. D.; Avouris, P. *J. Phys. Chem. B* **2001**, *105*, 11227. (b) Boukhvalov, D. W.; Katsnelson, M. I. *J. Am. Chem. Soc.* **2008**, *130*, 10697. (c) Barinov, A.; Malcioğlu, O. B.; Fabris, S.; Sun, T.; Gregoratti, L.; Dalmiglio, M.; Kiskinova, M. *J. Phys. Chem. C* **2009**, *113*, 9009. (d) Yan, J.-A.; Chou, M. Y. *Phys. Rev. B* **2010**, *82*, 125403. (e) Nourbakhsh, A.; Cantoro, M.; Klekachev, A. V.; Pourtois, G.; Vosch, T.; Hofkens, J.; van der Veen, M. H.; Heyns, M. M.; De Gendt, S.; Sels, B. F. *J. Phys. Chem. C* **2011**, *115*, 16619. (f) Radovic, L. R.; Suarez, A.; Vallejos-Burgos, F.; Sofo, J. O. *Carbon* **2011**, *49*, 4226. (g) Topsakal, M.; Şahin, H.; Ciraci, S. *Phys. Rev. B* **2012**, *85*, 155445. (h) Boukhvalov, D. W. *RSC Adv.* **2013**, *3*, 7150.

(8) (a) Wang, S.; Chia, P.-J.; Chua, L.-L.; Zhao, L.-H.; Png, R.-Q.; Sivaramakrishnan, S.; Zhou, M.; Goh, R. G.-S.; Friend, R. H.; Wee, A. T.-S.; Ho, P. K.-H. *Adv. Mater.* **2008**, *20*, 3440. (b) Yang, H.; Shan, C.; Li, F.; Han, D.; Zhang, Q.; Niu, L. *Chem. Commun.* **2009**, 3880.

(9) Johns, J. E.; Alaboson, J. M. P.; Patwardhan, S.; Ryder, C. R.; Schatz, G. C.; Hersam, M. C. *J. Am. Chem. Soc.* **2013**, *135*, 18121.

(10) Perdew, J. P.; Zunger, A. *Phys. Rev. B* **1981**, *23*, 5048.

(11) (a) Kresse, G.; Hafner, J. *Phys. Rev. B* **1993**, *47*, 558. (b) Kresse, G.; Furthmüller, J. *Phys. Rev. B* **1996**, *54*, 11169.

(12) (a) Li, X.; Cai, W.; An, J.; Kim, S.; Nah, J.; Yang, D.; Piner, R.; Velamakanni, A.; Jung, I.; Tutuc, E.; Banerjee, S. K.; Colombo, L.; Ruoff, R. S. *Science* **2009**, *324*, 1312. (b) Gao, L.; Guest, J. R.; Guisinger, N. P. *Nano Lett.* **2010**, *10*, 3512. (c) Lim, H.; Jung, J.; Yang, H. J.; Kim, Y. *Adv. Mater. Interfaces* **2014**, *1*, 1300080.

(13) Bae, S.; Kim, H.; Lee, Y.; Xu, X.; Park, J.-S.; Zheng, Y.; Balakrishnan, J.; Lei, T.; Kim, H. R.; Song, Y. I.; Kim, Y.-J.; Kim, K. S.; Özyilmaz, B.; Ahn, J.-H.; Hong, B. H.; Iijima, S. *Nat. Nanotechnol.* **2010**, *5*, 574.

(14) (a) Giovannetti, G.; Khomyakov, P. A.; Brocks, G.; Karpan, V. M.; van den Brink, J.; Kelly, P. J. *Phys. Rev. Lett.* **2008**, *101*, 026803. (b) Gong, C.; Lee, G.; Shan, B.; Vogel, E. M.; Wallace, R. M.; Cho, K. *J. Appl. Phys.* **2010**, *108*, 123711.

(15) Henkelman, G.; Uberuaga, B. P.; Jónsson, H. *J. Chem. Phys.* **2000**, *113*, 9901.

(16) (a) Manz, T. A.; Sholl, D. S. *J. Chem. Theory Comput.* **2010**, *6*, 2455. (b) Manz, T. A.; Sholl, D. S. *J. Chem. Theory Comput.* **2012**, *8*, 2844.

(17) The interfacial interaction energies (distances) between graphene layer and metal substrate before O adsorption are calculated to be 11 (3.27) and 84 (2.07) meV (Å) per C atom for Cu(111) and Ni(111), respectively.